

Cite this: *Food Funct.*, 2026, **17**, 3248

## *Ligilactobacillus salivarius* Li01 enhances gut microbiota-derived indole-3-propionic acid to alleviate 5-fluorouracil-induced diarrhea in mice

Pengyu Yin,<sup>†a,b</sup> Bo Qiu,<sup>†a</sup> Lwan Xu,<sup>a</sup> Siyuan Xie,<sup>a</sup> Shuobo Zhang,<sup>a</sup> Jingyi Zhang,<sup>a</sup> Björn Berglund,<sup>c</sup> Mingfei Yao <sup>\*a,b,d</sup> and Lanjuan Li <sup>\*a,b,d</sup>

As a widely applied chemotherapeutic agent, 5-fluorouracil (5-FU) frequently causes significant gastrointestinal side effects, particularly diarrhea, a process in which the gut microbiome serves as a crucial mediator. In this study, we evaluated the effect of oral administration of *Ligilactobacillus salivarius* Li01 (Li01) on 5-FU-induced intestinal mucositis in mice. We discovered that intake of Li01 was associated with alleviated diarrheal symptoms by mitigating inflammation, reducing oxidative stress, and restoring intestinal barrier function. Moreover, transcriptome analysis revealed that the Th17 signaling pathway was significantly suppressed. We also confirmed the essential contribution of the gut microbiota in mediating these effects, since the protective benefits of Li01 were not observed when the gut microbiota was depleted by antibiotics. Furthermore, administration of Li01 markedly increased the production of indole-3-propionic acid (IPA) by the gut microbiota. This key molecule was shown to contribute to the protection against 5-FU-associated diarrhea by activating the pregnane X receptor (PXR). Additionally, a close correlation was identified between IPA levels and the abundance of two bacterial species that form a mutualistic relationship with strain Li01: *Lactobacillus reuteri* and *Lactobacillus johnsonii*. In conclusion, our study demonstrates that Li01 alleviates 5-FU-induced diarrhea and microbiota dysbiosis by enhancing gut microbiota-derived IPA, supporting its potential as a probiotic.

Received 6th January 2026,  
Accepted 2nd March 2026

DOI: 10.1039/d6fo00050a

rsc.li/food-function

## Introduction

Chemotherapy is a critical tool in the treatment of malignancies. A key limitation of chemotherapy, however, is that the treatment can adversely affect normal cells, particularly by impacting rapidly renewing cell types such as the mucosal cells of the intestines, oral cavity, and stomach.<sup>1</sup> 5-FU is a first-line chemotherapeutic agent for cancer,<sup>2</sup> which has been shown to substantially increase cure and survival rates for patients with colon cancer.<sup>3</sup> However, 5-FU therapy induces severe adverse effects in 50–80% of patients, most notably intestinal mucositis, which presents as diarrhea, nausea, vomiting, and severe infections.<sup>4,5</sup> These adverse effects are

some of the primary reasons for treatment discontinuation, severely undermining the effectiveness of chemotherapy.<sup>6</sup> Despite being a significant concern in the treatment of cancer, the underlying mechanism of 5-FU-induced intestinal mucositis has not been fully elucidated.<sup>7</sup> Moreover, very few drugs can mitigate 5-FU-associated diarrhea, making the development of effective and safe treatment methods critically important.

The gut microbiota engages in a symbiotic association with the host and is described as an “accessory organ” that contributes to immune homeostasis, metabolic processes, and other physiological and pathological functions.<sup>8,9</sup> The administration of 5-FU markedly compromises the abundance and variety of the bacterial community.<sup>10</sup> Research has shown that 5-FU-induced impairment of the mucosal immune system in mice results in an increased abundance of *Pseudomonas aeruginosa*, consequently increasing host susceptibility to secondary pulmonary infection.<sup>11</sup> This evidence suggests that gut microbiota dysbiosis is closely associated with 5-FU-induced mucositis. However, it remains unknown which specific taxa of the gut microbiota are responsible for the toxic side effects associated with 5-FU chemotherapy.<sup>12</sup> Furthermore, the complex interplay between 5-FU-triggered intestinal dysbiosis and the host has not been well characterized.

<sup>a</sup>State Key Laboratory for Diagnosis and Treatment of Infectious Diseases, National Clinical Research Center for Infectious Diseases, China-Singapore Belt and Road Joint Laboratory on Infection Research and Drug Development, National Medical Center for Infectious Diseases, Collaborative Innovation Center for Diagnosis and Treatment of Infectious Diseases, The First Affiliated Hospital, Zhejiang University School of Medicine, Hangzhou, China. E-mail: ljli@zju.edu.cn, mingfei@zju.edu.cn

<sup>b</sup>Yuhang Institute for Collaborative Innovation and Translational Research in Life Sciences and Technology, Hangzhou, China

<sup>c</sup>Department of Cell and Molecular Biology, Uppsala University, Uppsala, Sweden

<sup>d</sup>Jinan Microecological Biomedicine Shandong Laboratory, Jinan, China

<sup>†</sup>These authors contributed equally to this study.



The term “probiotics” refers to living microorganisms which, upon administration in sufficient dosages, have a scientifically beneficial impact on human well-being.<sup>13</sup> Probiotic supplementation alters the intestinal microecological landscape and participates in the synthesis of various metabolites, such as short-chain fatty acids (SCFAs), branched-chain amino acids (BCAAs), and secondary bile acids.<sup>14</sup> Therapeutic applications of probiotics are becoming increasingly common, especially for treatment of gastrointestinal disorders, such as inflammatory bowel disease and irritable bowel syndrome.<sup>15,16</sup> Specific probiotics, such as *Lactobacillus delbrueckii* CIDCA 133 and *Lactobacillus rhamnosus* FLRH93, have been reported to be effective at alleviating intestinal mucositis caused by 5-FU in mice.<sup>17,18</sup> *Ligilactobacillus salivarius* Li01 is a probiotic isolated from feces of healthy adults in our laboratory. Previous studies have shown that Li01 ameliorates loperamide-induced constipation in mice *via* modulation of the 5-HT pathway.<sup>19</sup> In addition, Li01 has shown potential as a probiotic in alleviating hepatic encephalopathy secondary to acute liver injury.<sup>20</sup> However, the effect and mechanism of Li01 on diarrhea caused by 5-FU have not been studied yet.

In this study, we investigated the efficiency of Li01 on 5-FU-induced intestinal mucositis in mice. Li01 administration alleviated diarrhea by mitigating inflammation, reducing oxidative damage, and restoring intestinal barrier function. Antibiotic treatment validated that the protective effects of Li01 were mediated by the gut microbiota. Mechanistically, Li01 exerted its benefits by elevating the level of gut microbiota-derived IPA, which in turn activated the PXR. Our findings highlight IPA as a crucial microbiota-derived metabolite that mediates the beneficial effects of Li01, thereby contributing to the potential use of Li01 as a probiotic for the management of 5-FU-induced diarrhea.

## Materials and methods

### Li01 cultivation

*Ligilactobacillus salivarius* Li01 (CGMCC 7045), initially isolated from feces of healthy adults in our laboratory, was cultured in MRS broth (OXOID, Hampshire, UK) at 37 °C for 24 h under anaerobic conditions. After cultivation, the bacteria were harvested by centrifugation at 4000 rpm for 10 min. The bacterial precipitate was then washed twice with phosphate-buffered saline (PBS) and resuspended in PBS to a density of  $5 \times 10^9$  CFU per mL before further use.<sup>21</sup>

### Animal experiments

Specific pathogen-free male C57BL/6 mice (6 weeks old) were purchased from Ziyuan Company (Hangzhou, China). Mice were raised in an environment under standard room temperature conditions, a 12 h light/12 h dark cycle, and free access to water and food. The mice were acclimated for a week before subsequent experiments. All animal-related experiments were conducted according to ethical policies and procedures approved by the Institutional Animal Care and Use Committee

of The First Affiliated Hospital, Zhejiang University School of Medicine (reference no.: 2025-201).

To elucidate the role of Li01 in the context of 5-FU-induced diarrhea, 24 C57 mice were randomly assigned to three groups ( $n = 8$  per group): the negative control (NC) group, the 5-fluorouracil (PC) group, and the Li01 + 5-FU (Li01) group. Mice in the Li01 group were orally administered 0.2 mL of fresh Li01 suspension per day for 14 days, while mice in the NC and PC groups were orally administered 0.2 mL of PBS daily. From Day 10 to Day 14, mice in the PC and Li01 groups were daily injected intraperitoneally with 50 mg per kg body weight 5-FU (Sigma-Aldrich, St. Louis, USA), whereas mice in the NC group were injected with PBS daily.<sup>22</sup> Throughout the experiment, body weight and the diarrhea status were monitored daily. Diarrhea scores were evaluated according to Table S1. All mice were euthanized on Day 15, after which blood, intestinal tissue, and intestinal contents were collected and stored.

To explore whether the effect of Li01 on 5-FU-triggered intestinal mucositis is dependent on the gut microbiota, we randomly divided 24 mice into 4 groups ( $n = 6$  per group): the negative control (NC) group, the antibiotics (Abx) group, the Abx + 5-FU (APC) group, and the Abx + Li01 + 5-FU (ALi01) group. All mice except mice in the NC group were treated with an antibiotic solution containing 1 g L<sup>-1</sup> ampicillin, 1 g L<sup>-1</sup> metronidazole, 1 g L<sup>-1</sup> neomycin sulfate, and 0.5 g L<sup>-1</sup> vancomycin (Sigma-Aldrich, St. Louis, USA) added to drinking water for 14 days. Subsequently, mice in all groups were switched to normal drinking water. From Day 14 to Day 27, mice in the Li01 group were orally administered 0.2 mL day<sup>-1</sup> Li01 suspension, while mice in the remaining groups were orally administered 0.2 mL day<sup>-1</sup> PBS. Mice in the APC and ALi01 groups were administered 5-FU solution *via* intraperitoneal injection daily from Day 23 to Day 27, whereas mice in the NC and Abx groups received injections of PBS. On Day 28, all mice were sacrificed, and samples of blood, colon, and intestinal contents were collected for subsequent analysis.

To examine whether the antibiotic cocktail has a direct effect on Li01's function, 12 mice were allocated to 2 groups ( $n = 6$  per group): the Abx + PBS group and the Abx + Li01 group. All mice received the antibiotic regimen *via* their drinking water for 14 days. Subsequently, all mice were switched to regular drinking water. From Day 14 to Day 24, mice in the Abx + Li01 group were orally administered 0.2 mL day<sup>-1</sup> Li01 suspension, while mice in the Abx + PBS group were orally administered 0.2 mL day<sup>-1</sup> PBS. Fecal samples were collected on Days 1, 7, 14, 19, and 24. The fecal samples were resuspended and diluted in PBS, plated onto MRS agar (OXOID, Hampshire, UK) and incubated anaerobically at 37 °C for 48 hours. Colony-forming units (CFUs) were calculated to assess the colonization of Li01.<sup>23</sup> All mice were euthanized on Day 24, after which blood, intestinal tissue, and intestinal contents were collected.

To investigate the protective effect of the key metabolite IPA, 24 mice were allocated to 4 groups ( $n = 6$  per group): the negative control (NC) group, the 5-fluorouracil (PC) group, the 5-FU + IPA10 (IPA10) group, and the 5-FU + IPA20 (IPA20)



group. In the IPA10 and IPA20 groups, mice were orally administered IPA (Sigma-Aldrich, St. Louis, USA) for 11 days at concentrations of 10 mg kg<sup>-1</sup> and 20 mg kg<sup>-1</sup>, respectively.<sup>24</sup> All mice except mice in the NC group were intraperitoneally injected with 5-FU daily from Day 7 to Day 11. On Day 12, blood, intestinal tissue, and intestinal contents were collected after sacrifice.

### Histological analysis

Colon tissues from sacrificed mice were fixed in 4% paraformaldehyde (Biosharp, Beijing, China), embedded in paraffin, and sectioned. For histological evaluation, sections were subjected to Hematoxylin and Eosin (HE) and Alcian Blue/Periodic Acid-Schiff (AB-PAS) staining to assess the general morphology and goblet cells, respectively. Immunofluorescence staining of ZO-1 was performed using the specific antibody (Proteintech, Chicago, USA). Additionally, immunohistochemical staining of myeloperoxidase (MPO), occludin, and ZO-1 was conducted by using the corresponding antibodies (Proteintech, Chicago, USA). All staining procedures followed standardized protocols, including antigen retrieval and blocking, incubation with specific primary antibodies, and appropriate secondary antibodies. Quantitative analysis was performed by using ImageJ software.

### Transmission electron microscopy (TEM)

Distal colon segments from sacrificed mice were removed and immediately placed in a 2.5% glutaraldehyde solution (Solarbio, Beijing, China) for 24 hours. Then, the samples were fixed with 1% osmic acid, fixed/stained with 2% uranium acetate, dehydrated with gradient ethanol, embedded, and sliced. Finally, the processed tissues were observed by using a Tecnai G2 Spirit transmission electron microscope (Thermo Fisher Scientific, Waltham, USA).

### Serum cytokines and IPA measurement

Serum from sacrificed mice was obtained by centrifuging the collected blood at 4000g for 15 min. Serum cytokines, including IL-6, IL-10, IL-1 $\beta$ , IL-17A, IFN- $\gamma$ , and TNF- $\alpha$ , were assessed by using a Mouse Cytokine 6-Plex Panel (Bio-Rad, California, USA) following the manufacturer's instructions. Serum IPA levels were measured by using an ELISA kit (COIBO BIO, Shanghai, China) according to the manufacturer's guidelines.

### Estimation of intestinal oxidative stress levels

The protein concentration of intestinal tissues from sacrificed mice was quantified with a BCA Protein Assay Kit (Beyotime, Shanghai, China). Then, the content of malondialdehyde (MDA) and the activity of superoxide dismutase (SOD) were measured by using the corresponding detection kit (Beyotime, Shanghai, China).

### Cell experiments

The human colon adenocarcinoma Caco-2 cell line was purchased from ATCC (Manassas, VA, USA) and cultured in Dulbecco's modified Eagle's medium (DMEM, Gibco, MD,

USA) supplemented with 10% fetal bovine serum (FBS, Gibco, MD, USA) and 1% penicillin/streptomycin (Beyotime, Shanghai, China) at 37 °C under 5% CO<sub>2</sub>.<sup>25</sup>

To evaluate the sensitivity of Caco-2 to IPA, Caco-2 cells were seeded in 96-well plates. After incubation for 24 h, the cells were exposed to 0  $\mu$ M, 5  $\mu$ M, 25  $\mu$ M, 50  $\mu$ M, 100  $\mu$ M, 200  $\mu$ M, and 500  $\mu$ M IPA for 24 h. Then, a CCK8 kit (Beyotime, Shanghai, China) was used to measure the cell viability following the manufacturers' instructions.

To explore the effects of IPA on 5-FU-induced cellular injury, Caco-2 cells were divided into 4 groups: the control group, the 5-FU group, the 5-FU + IPA group, and the 5-FU + IPA + ketoconazole (KTZ) group. The concentrations used were as follows: 5-FU at 10  $\mu$ M, IPA at 50  $\mu$ M, and the PXR antagonist ketoconazole (Sigma-Aldrich, St. Louis, USA) at 10  $\mu$ M.<sup>26,27</sup> Following a 24 hour treatment, cells were harvested for real-time qPCR analysis.

### In vitro probiotic culture experiments

To investigate whether Li01, *Lactobacillus reuteri*, and *Lactobacillus johnsonii* can convert tryptophan into IPA in monoculture or co-culture, the following experiment was conducted. To provide sufficient substrate for bioconversion, MRS liquid broth was supplemented with L-tryptophan (Macklin, Shanghai, China) at a concentration of 5 g L<sup>-1</sup>. The medium was then divided into six groups inoculated with different probiotics as follows: no probiotics (MRS), Li01 (Li01), *Lactobacillus reuteri* LR08 (L.r.), *Lactobacillus johnsonii* 6084 (L.j.), Li01 + *L. reuteri* LR08 (Li01 + L.r.), and Li01 + *L. johnsonii* 6084 (Li01 + L.j.). Each strain was inoculated at an initial concentration of 1  $\times$  10<sup>7</sup> CFU per mL.<sup>28</sup> All cultures were incubated anaerobically at 37 °C for 48 h. After incubation, the cultures were centrifuged at 4000 rcf for 10 min, and the resulting supernatants were collected for subsequent analysis.

### Real-time quantitative PCR

The RNA of intestinal tissue from sacrificed mice and Caco-2 cells was extracted by using an RNeasy Kit (Qiagen, Hilden, Germany). Subsequently, cDNA was synthesized using PrimeScript RT Master Mix (Takara, Kusatsu, Japan). The relative gene expression levels were determined with a QuantStudio 5 Real-Time PCR system (Thermo Fisher Scientific, Waltham, MA) by using TB Green Premix Ex Taq (Takara, Kusatsu, Japan). Relative gene expression was calculated using the 2<sup>- $\Delta\Delta$ CT</sup> method, and GAPDH was used as an internal reference. Primers are presented in Table S2.

### 16S rRNA gene sequencing

Following the manufacturer's guidelines, total bacterial DNA was isolated from murine fecal samples by using a DNeasy PowerSoil kit (Qiagen) and the quality and concentration were determined using 1.0% agarose gel electrophoresis and a NanoDrop ND-2000 spectrophotometer (Thermo Scientific). The V3-V4 variable region of the 16S rRNA gene was amplified by using specific primers.<sup>29</sup> Following PCR amplification, purification, and quantification, equal amounts of the amplicons



were pooled and subjected to sequencing on an Illumina NovaSeq 6000 system. Subsequent bioinformatic processing of the raw FASTQ files was performed to analyze the sequence data.

### Transcriptome sequencing

Colon tissue total RNA from sacrificed mice was isolated as outlined previously.<sup>30</sup> Following purification, enrichment, and fragmentation of mRNA, sequencing libraries were constructed with a TruSeq Stranded mRNA LT Sample Prep Kit (Illumina, CA, USA). The libraries were subjected to paired-end sequencing (150 bp) on an Illumina NovaSeq 6000 platform. Raw sequencing reads were processed to yield high-quality clean data. Principal component analysis (PCA) was performed by using R (v3.2.0). Differentially expressed genes (DEGs) were identified by DESeq2, and significantly enriched KEGG pathways were identified in R (v3.2.0). Gene Set Enrichment Analysis (GSEA) was implemented *via* the GSEA software platform.

### Untargeted metabolomic analysis of intestinal contents

Untargeted metabolomic profiling of murine colonic content samples was carried out as previously reported.<sup>31</sup> In brief, colonic contents (50 mg) were resuspended in pre-chilled 80% methanol and vortexed. The mixture was incubated on ice for 5 min and centrifuged at 20 000g at 4 °C for 20 min. The supernatant was diluted with LC-MS grade water to a final methanol concentration of 53%, followed by a second centrifugation. The supernatant was subjected to UHPLC-MS/MS analysis with raw data processed in Compound Discoverer 3.1 for peak alignment and quantification. Peak intensities were normalized to total spectral intensity, and metabolites were identified by matching against the mzVault, mzCloud, and MassList databases. Annotation was performed by using KEGG, HMDB, and LIPIDMaps. Multivariate analyses including PLS-DA were conducted in metaX. Differential metabolites were defined as those with variable importance in projection (VIP) >1 and  $p < 0.05$ . Clustering heatmaps were plotted by using the Pheatmap package in R language after z-score normalization of metabolite intensities.

### IPA-targeted metabolomics

IPA was extracted from murine feces using a two-step sequential extraction with ultrapure water and methanol. For the probiotic culture medium, proteins were precipitated by mixing the medium with ice-cold methanol. All samples were then sonicated, vortexed, and centrifuged, and the supernatants were dried using a centrifugal vacuum concentrator (Labconco, USA). The method for quantifying IPA was based on the separation capabilities of Ultra-High Performance Liquid Chromatography (UPLC) and the high sensitivity detection characteristics of Mass Spectrometry (MS). Using an external standard method, IPA was quantitatively analyzed. A calibration curve was established based on the peak area of the target compound and the concentration of the standard, allowing for the calculation of IPA content in the samples.

### Statistical analysis

Statistical analyses were performed by using IBM SPSS Statistics 22.0 and GraphPad Prism 10.1.2. Data normality was assessed with the Shapiro-Wilk test. Group comparisons were performed using Student's *t*-test or Mann-Whitney *U* test (for two groups), and ordinary ANOVA or Brown-Forsythe/Welch ANOVA (for multiple groups), as appropriate. Correlation between microbiota and IPA was analyzed by Pearson correlation analysis. Data are presented as mean  $\pm$  SEM, and differences with a *P* value <0.05 were recognized as statistically significant.

## Results

### Li01 conferred protection against 5-FU-triggered intestinal inflammation and diarrhea

To investigate the effect of Li01 on diarrhea caused by 5-FU, the following procedures were performed in mice (Fig. 1A). Mice treated with 5-FU exhibited pronounced body weight loss ( $P < 0.001$ ) and higher diarrhea scores ( $P < 0.001$ ) compared to mice in the NC group, accompanied by macroscopic observations of watery feces (Fig. 1B and C). However, these manifestations were substantially mitigated by oral gavage of Li01. In addition, administration of Li01 significantly ameliorated 5-FU-induced colonic shortening ( $P < 0.001$ ) (Fig. 1D), while no significant effect was observed on the length of the small intestine ( $P > 0.05$ ) (Fig. S1A). In line with the reduction in colon length, HE staining and MPO immunohistochemistry revealed that 5-FU inflicted severe damage to the colonic architecture, characterized by crypt loss, epithelial erosion, submucosal edema and neutrophil infiltration, all of which were improved by Li01 treatment (Fig. 1E). Quantitative analysis of MPO immunohistochemistry (Fig. S1B) revealed a significant reduction in MPO-positive cell counts in the Li01 group compared to the PC group. To assess systemic and local inflammation, levels of key cytokines were measured. 5-FU administration significantly elevated the serum concentrations of IL-1 $\beta$ , IL-6, TNF- $\alpha$ , and IL-17A (Fig. 1F), and concomitantly increased the colonic expression of IL-6, TNF- $\alpha$ , and IL-1 $\beta$  (Fig. S1C). Compared to the PC group, the levels of these pro-inflammatory factors were lower following Li01 administration. Additionally, Li01 increased the concentration of the anti-inflammatory cytokine IL-10 relative to the PC group (Fig. 1G). As shown in Fig. 1H, Li01 counteracted 5-FU-induced oxidative stress, with elevated SOD activity ( $P < 0.01$ ) and reduced MDA levels ( $P < 0.001$ ). Collectively, these data demonstrate that Li01 effectively attenuated 5-FU-induced diarrhea by mitigating inflammation and oxidative stress.

### Li01 improved 5-FU-induced intestinal barrier damage and reversed microbiome dysbiosis in mice

In order to investigate the impact of 5-FU on the intestinal barrier, key components including the microvilli, goblet cells, and tight junction proteins were examined. Analysis with TEM allowed identification of shortened, ruptured, and sparse



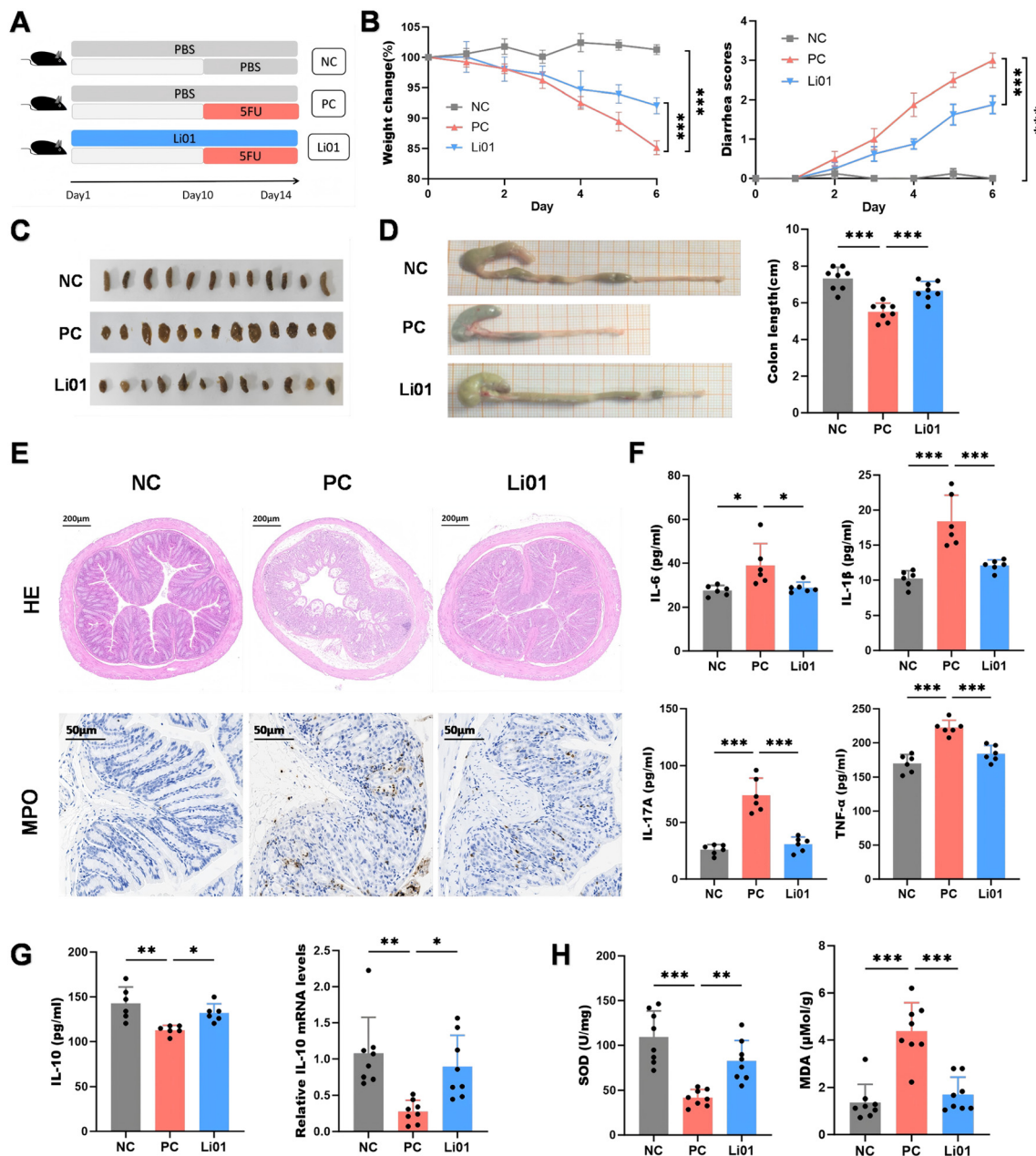


**Fig. 1** LiO1 alleviated 5-FU-induced diarrhea in mice. (A) Study design of the LiO1 intervention experiment. (B) Percentage of initial body weight and diarrhea scores of mice following 5-FU administration. (C) Fecal form on the last day. (D) Representative photos of the colon (left) and colon length (right) from mice on the final day. (E) Representative images of HE staining and immunohistochemical staining of MPO in colon tissues. (F) The levels of IL-6, IL-1 $\beta$ , IL-17A, and TNF- $\alpha$  in serum. (G) The level of IL-10 in serum and its relative expression in colon tissues. (H) SOD activity and MDA concentration in colon tissues. Data are presented as mean  $\pm$  SEM. \* $P$  < 0.05, \*\* $P$  < 0.01, \*\*\* $P$  < 0.001.

intestinal microvilli among mice in the PC group, whereas the LiO1 group appeared denser and more intact (Fig. 2A). Additionally, AB-PAS staining revealed that, compared to the NC group, 5-FU treatment greatly depleted the intestinal goblet cell population ( $P$  < 0.001) (Fig. 2A and B). However, the administration of LiO1 resulted in a higher number of goblet cells ( $P$  < 0.001) compared to the PC group. Moreover, colonic immunofluorescence staining revealed a higher density of ZO-1 in the LiO1 group than in the PC group (Fig. 2A).

Likewise, pretreatment with LiO1 elevated the relative expression levels of occludin, claudin-1, and ZO-1 in the colon (Fig. S2A). To explore alterations in the gut microbiota, 16S ribosomal RNA gene amplicon sequencing was utilized. Microbial  $\alpha$ -diversity was markedly restored in the LiO1 group compared to the PC group, as reflected by the Observed species ( $P$  < 0.05) and Chao1 index ( $P$  < 0.01) (Fig. 2C). The  $\beta$ -diversity, assessed by PCoA (Fig. 2D), showed that 5-FU-treated mice clustered separately from mice in the NC group,



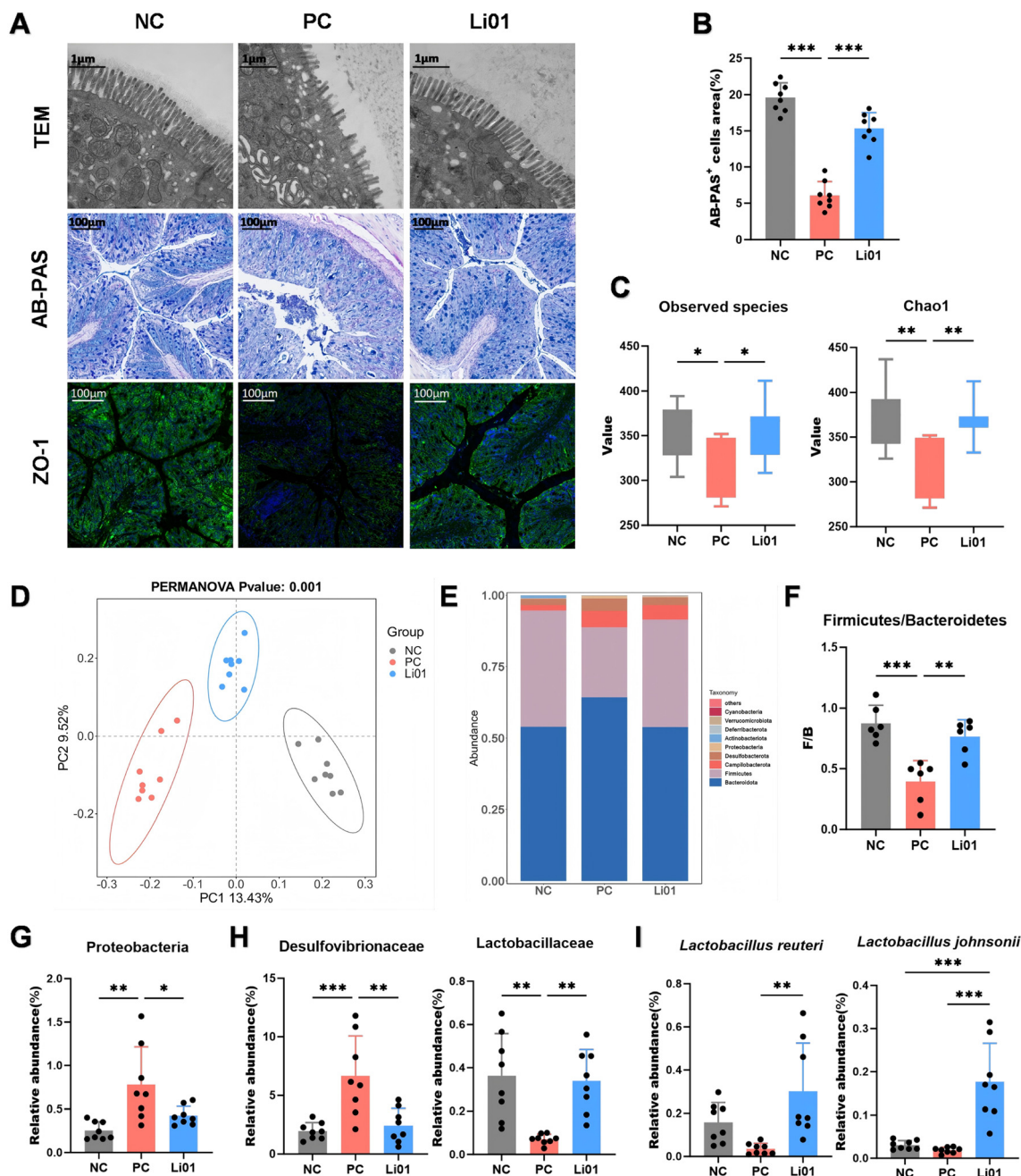


**Fig. 2** LiO1 protected the gut barrier and microbiota from 5-FU damage in mice. (A) Representative images of TEM, AB-PAS staining and immunofluorescence staining of ZO-1 in colon tissues. (B) Quantification of AB-PAS-positive cell area. (C) Alpha diversity indices (Observed species and Chao1). (D) Principal coordinate analysis (PCoA) of the gut microbiota. (E) Relative abundance of bacteria at the phylum level. (F) Firmicutes to Bacteroidetes (F/B) ratio. (G) Relative abundance of Proteobacteria at the phylum level. (H) Relative abundance of Desulfovibrionaceae and Lactobacillaceae at the family level. (I) Relative abundance of *Lactobacillus reuteri* and *Lactobacillus johnsonii* at the species level. Data are presented as mean  $\pm$  SEM. \* $P < 0.05$ , \*\* $P < 0.01$ , \*\*\* $P < 0.001$ .

indicating a shift in microbiota composition. However, this shift was attenuated by the administration of LiO1. The profile of the gut microbiome at the phylum level is presented in Fig. 2E. At the phylum level, the Firmicutes/Bacteroidetes ratio ( $P < 0.001$ ) was significantly lower in the PC group than in the NC group (Fig. 2F). Compared to the PC group, the LiO1 group exhibited a significantly higher F/B ratio ( $P < 0.01$ ).

Furthermore, LiO1 reversed the 5-FU-induced elevation in the abundance of Proteobacteria ( $P < 0.05$ ) (Fig. 2G). At the family level, in contrast to 5-FU treatment, which increased the abundance of Desulfovibrionaceae while reducing the abundance of Lactobacillaceae, LiO1 administration produced the opposite effect, effectively suppressing Desulfovibrionaceae ( $P < 0.01$ ) and elevating Lactobacillaceae ( $P < 0.01$ ) levels (Fig. 2H). At the



species level, the abundance of *L. reuteri* ( $P < 0.01$ ) and *L. johnsonii* ( $P < 0.001$ ) was significantly higher in the Li01 group than in the PC group (Fig. 2I).

### Li01 supplementation increased the level of microbiota-derived indole-3-propionic acid in 5-FU-treated mice

Transcriptome analysis of murine colon tissue identified 369 significantly upregulated and 755 significantly downregulated DEGs among mice in the Li01 group compared to mice in the PC group (Fig. S3A and B). As shown in Fig. S3C, the PCA plot showed clear separation among mice in the NC, PC, and Li01 groups. The top 10 downregulated pathways based on the KEGG analysis between the Li01 group and the PC group are shown in Fig. 3A. Notably, the Th17 cell differentiation pathway showed significant downregulation in the Li01 group compared to the PC group. The GSEA results show that Li01 significantly suppressed the Th17 cell differentiation, Th1 and Th2 cell differentiation and cytokine–cytokine receptor interaction pathways (Fig. 3B). To elucidate the underlying mechanism by which Li01 conferred protection in 5-FU-treated mice, LC-MS was employed to analyze the metabolic profiles of colonic contents and a total of 1232 metabolites were identified. The PLS-DA showed distinct clustering of metabolites among the three groups (Fig. 3C). Subsequently, the top 20 differential metabolites between the Li01 and the PC groups were screened (Fig. 3D). Li01 supplementation resulted in the downregulation of 11 metabolites and the upregulation of 9 metabolites. Of the 9 metabolites markedly elevated in the Li01 group, only IPA was microbiota-derived. IPA levels were subsequently analyzed in all three groups. The administration of 5-FU resulted in a decrease in the relative abundance of IPA in colonic contents and its concentration in serum (Fig. 3E and F). However, both parameters were significantly higher following Li01 intervention compared to the PC group. Expression levels of PXR and AhR, the primary receptors mediating the biological functions of IPA, were also analyzed.<sup>32</sup> Specifically, compared to the PC group, Li01 treatment significantly upregulated PXR expression ( $P < 0.05$ ), whereas the level of AhR ( $P > 0.05$ ) showed no obvious change (Fig. 3G).

### Gut microbiota mediated the protective function of Li01 against 5-FU-induced mucositis

To determine whether the protective effects of Li01 in 5-FU-treated mice are mediated by gut microbiota, an antibiotic cocktail was administered to deplete the gut microbiota in the Abx, APC, and ALi01 groups before gavage and intraperitoneal injection (Fig. 4A). As assessed from cultures of fecal samples on Day 14, antibiotic treatment resulted in a significantly lower bacterial burden compared to the NC group (Fig. S4A). During this experiment, 5-FU caused significant weight loss, diarrhea and shortened colon in the APC group, but treatment with Li01 failed to alleviate these symptoms (Fig. 4B and C). There was also no observable difference in the IL-6, TNF- $\alpha$ , IL-10 and IL-17A levels between the APC and ALi01 groups (Fig. 4D and Fig. S4B). Consistently, Li01's ability to counteract oxidative stress was abrogated in microbiota-depleted mice, as

it neither improved the decline of SOD activity nor alleviated the increase in MDA content triggered by 5-FU (Fig. S4C). In addition, combined assessment of colon tissue by HE staining and TEM revealed that mice administered with 5-FU showed marked epithelial erosion and loss, crypt damage, and villus disarray compared to mice in the Abx group (Fig. 4E). However, supplementation with Li01 did not ameliorate these pathological alterations. Similarly, MPO immunohistochemistry and its quantitative analysis (Fig. S4D and E) showed no significant difference in MPO-positive cell counts between the APC and ALi01 groups. Furthermore, analysis of tight junction proteins *via* immunohistochemistry (ZO-1, occludin) and gene expression (ZO-1, occludin, and claudin-1) confirmed that the protective effect of Li01 on the gut barrier was abrogated by antibiotic pretreatment (Fig. 4E and F). These results highlight that the presence of gut microbiota is a prerequisite for Li01 to exert its effects against 5-FU-induced mucositis. To rule out potential direct effects of the antibiotic cocktail on the viability of Li01, the Abx + PBS group and the Abx + Li01 group were set up, as shown in Fig. S5A. Following antibiotic application, the *Lactobacillus* content in the feces of both groups decreased significantly (Fig. S5B). From Day 14 to Day 24, the *Lactobacillus* content of the Abx + Li01 group showed a marked increase compared to the Abx + PBS group (Fig. S5B). This indicates that successful colonization of Li01 in the gut was achieved following antibiotic administration. No significant differences were observed between two groups in terms of colon length, colon HE staining, or the expression of IL-6, TNF- $\alpha$ , and occludin in the colon (Fig. S5C–E).

### IPA production was dependent on the gut microbiota

To further investigate the altered gut microbiota, we conducted 16S rRNA gene sequencing on fecal samples from mice subjected to antibiotic intervention. Comparison between the NC and Abx groups revealed that antibiotic pretreatment resulted in a significant decline in  $\alpha$ -diversity indices including Chao1 ( $P < 0.001$ ), Observed species ( $P < 0.001$ ), and Shannon index ( $P < 0.01$ ) (Fig. 5A). Interestingly, mice in the APC and ALi01 groups showed similar levels of  $\alpha$ -diversity. The F/B ratio ( $P > 0.05$ ) at the phylum level did not differ significantly between the APC and ALi01 groups (Fig. 5B). Given that Li01 administration significantly increased the abundance of *L. reuteri* and *L. johnsonii* in mice without antibiotic treatment, we next assessed whether the abundance of these two bacterial species would change in antibiotic-treated mice. Following antibiotic administration, Li01 failed to increase the abundance of *L. reuteri* ( $P > 0.05$ ) and *L. johnsonii* ( $P > 0.05$ ) at the species level (Fig. 5C). Targeted quantification of IPA in fecal samples and measurement of serum IPA levels were also performed; however, no significant difference in IPA concentrations between the ALi01 and APC groups could be observed (Fig. 5D). In mice receiving antibiotic water, 5-FU administration resulted in lower PXR mRNA levels, whereas mice treated with Li01 produced no obvious difference compared to the APC group (Fig. 5E). These results indicated that the gut microbiota is essential for IPA production. To test our hypothesis that *L. reuteri* and *L. johnsonii* are key contribu-



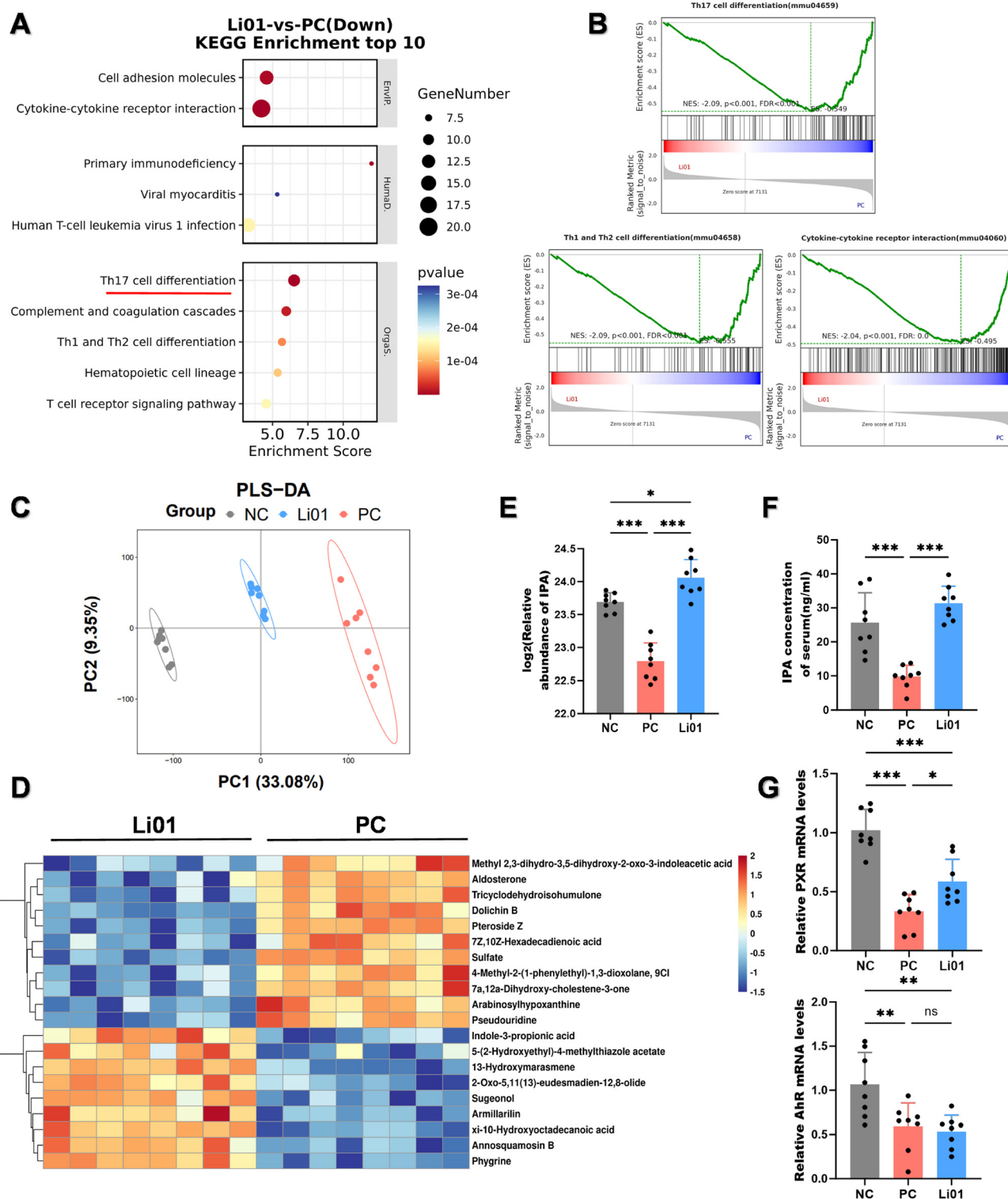


**Fig. 3** Li01 elevated indole-3-propionic acid in 5-FU-treated mice. (A) Top 10 enriched down-regulation pathways based on KEGG analysis in Li01 vs. PC. (B) Enriched signaling pathway using GSEA in Li01 vs. PC. (C) Partial least squares discrimination analysis (PLS-DA) plot of untargeted metabolomics from colonic contents. (D) Heatmap of the top 20 differentially abundant metabolites between the Li01 group and the PC group. (E) Relative abundance of IPA in colonic contents among the three groups. (F) Concentration of IPA in serum. (G) Relative colonic expression of the IPA target genes (PXR and AhR). Data are presented as mean  $\pm$  SEM. ns,  $P > 0.05$ ,  $*P < 0.05$ ,  $**P < 0.01$ ,  $***P < 0.001$ .



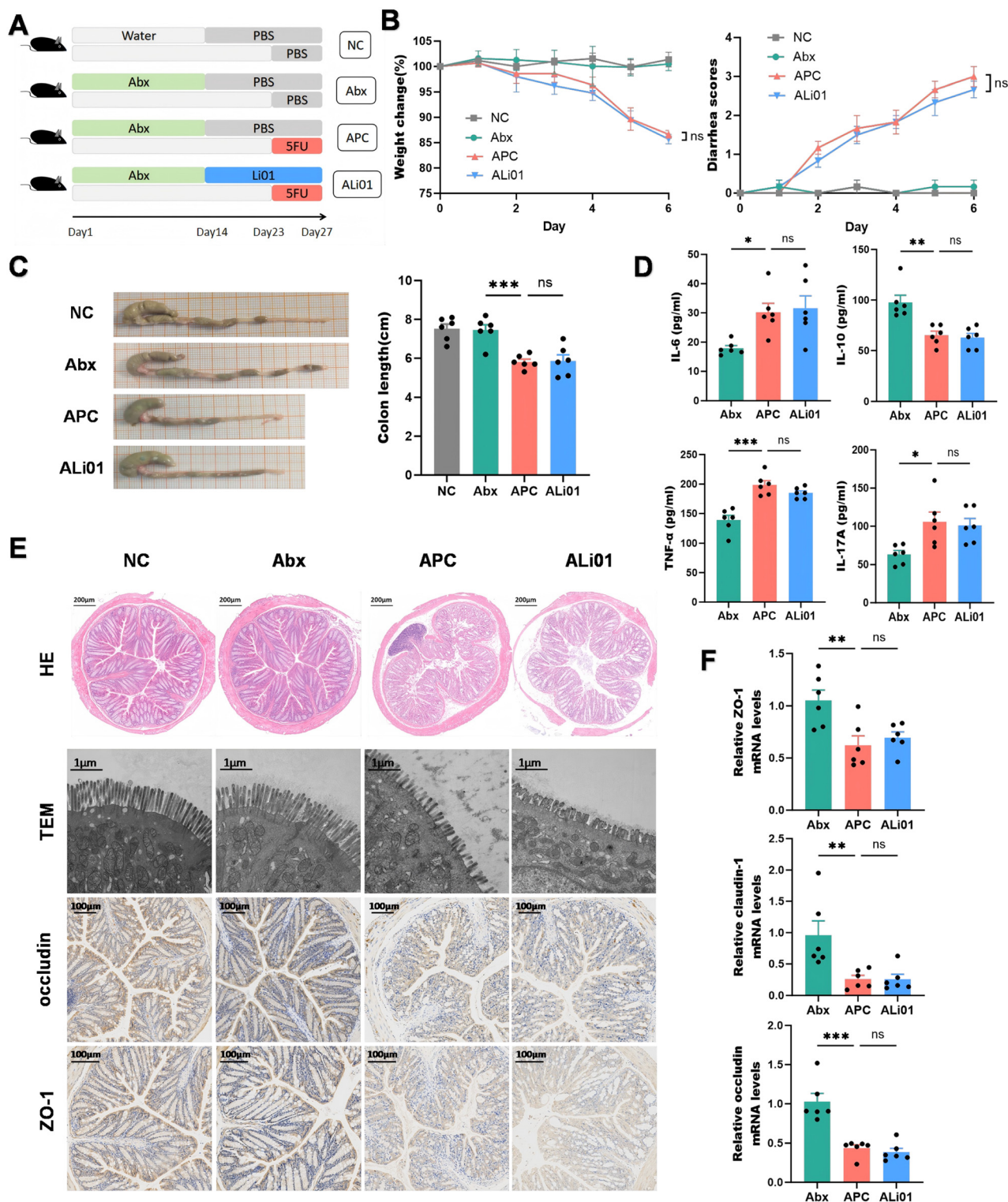


**Fig. 4** LiO1's anti-diarrheal effect against 5-FU was gut microbiota-dependent. (A) Study design of antibiotic administration experiment. (B) Body weight change and diarrhea scores after 5-FU administration. (C) Representative colon images (left) and quantitative analysis of colon length (right). (D) Cytokines in the serum, including IL-6, IL-10, TNF- $\alpha$ , and IL-17A. (E) Representative images of HE staining, TEM, occludin and ZO-1 immunohistochemical staining in colon tissues. (F) Relative expression of ZO-1, claudin-1, and occludin in colon tissues. Data are presented as mean  $\pm$  SEM. ns,  $P > 0.05$ , \* $P < 0.05$ , \*\* $P < 0.01$ , \*\*\* $P < 0.001$ .



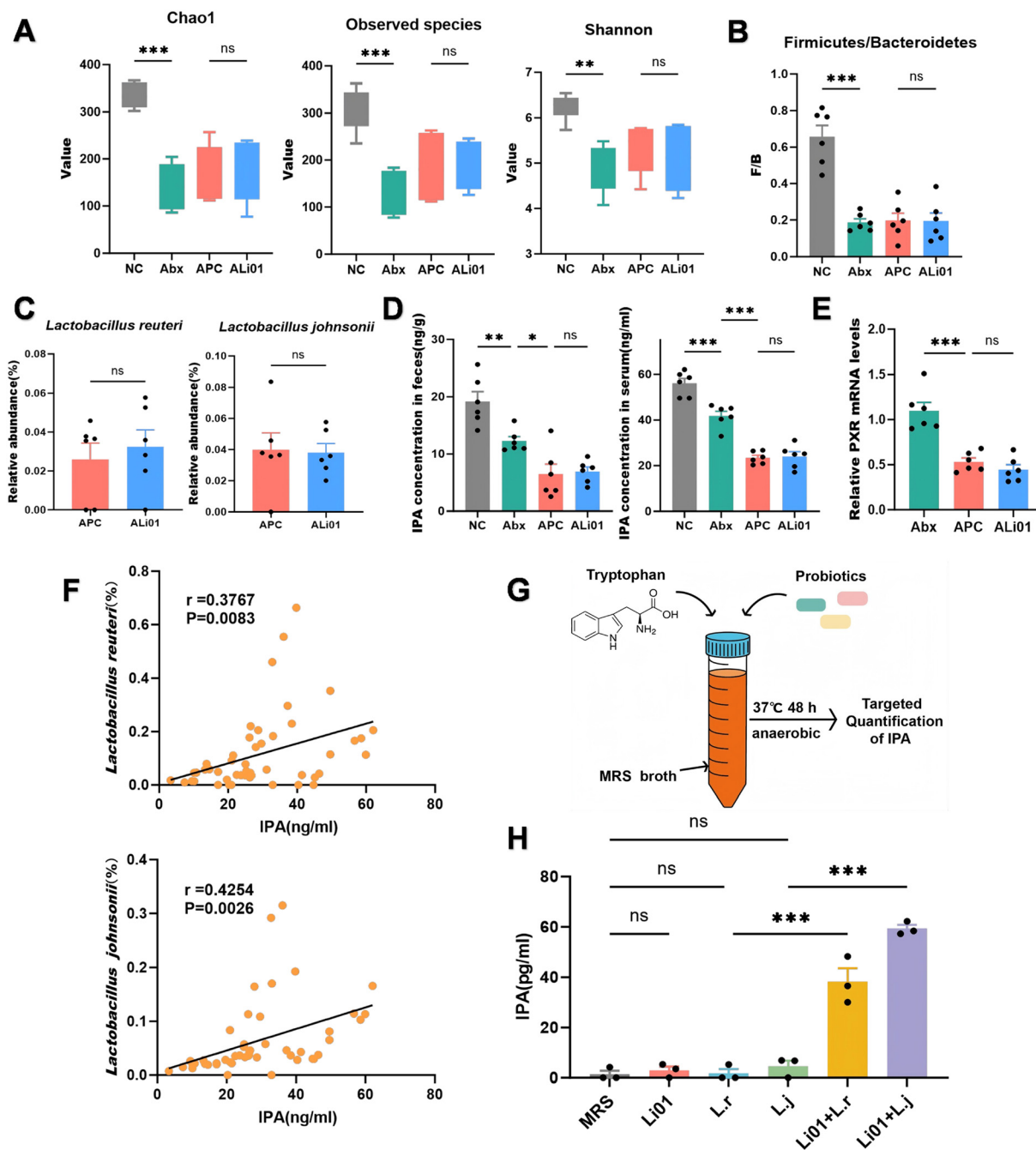


**Fig. 5** IPA production was mediated by the gut microbiota. (A) The  $\alpha$ -diversity including Chao1, Observed species, and Shannon index of the gut microbiota. (B) F/B ratio. (C) Relative abundance of *Lactobacillus reuteri* and *Lactobacillus johnsonii*. (D) IPA levels in feces obtained by targeted metabolomics and in serum by ELISA. (E) Relative colonic PXR mRNA expression level. (F) Correlation analysis of IPA levels with the relative abundance of *Lactobacillus reuteri* and *Lactobacillus johnsonii*. (G) *In vitro* culture procedure. (H) IPA content in the probiotic culture supernatant. Data are presented as mean  $\pm$  SEM. ns,  $P > 0.05$ , \* $P < 0.05$ , \*\* $P < 0.01$ , \*\*\* $P < 0.001$ .

tors to host IPA levels, we performed a correlation analysis. As illustrated in Fig. 5F, correlation analysis showed that IPA concentration was positively associated with the abundance of *L. reuteri* ( $P = 0.0083$ ,  $r = 0.3767$ ) and the abundance of *L. johnsonii* ( $P = 0.0026$ ,  $r = 0.4254$ ). To further explore the role of the microbiota in IPA production, *in vitro* cultures were conducted (Fig. 5G). The IPA levels in the culture supernatant of the

Li01 group, the *L. reuteri* group, and the *L. johnsonii* group showed no significant difference compared to the MRS control group (Fig. 5H), indicating that Li01, *L. reuteri*, and *L. johnsonii* were individually incapable of converting tryptophan to IPA. However, a significant increase in IPA generation was observed in co-cultures of Li01 with *L. reuteri* ( $P < 0.001$ ) as well as Li01 with *L. johnsonii* ( $P < 0.001$ ).



## Administration of IPA alleviated 5-FU-induced intestinal mucositis

The effect of IPA on 5-FU-induced diarrhea in mice was investigated by administering mice with IPA (10 mg kg<sup>-1</sup> or 20 mg kg<sup>-1</sup>) or PBS *via* gavage for 11 days (Fig. 6A). All mice except those in the NC group were intraperitoneally injected with 5-FU daily from Day 7 to Day 11. Compared to mice in the PC group, mice in the IPA-treated groups, particularly at the 20 mg kg<sup>-1</sup> dose, showed significantly attenuated mucositis-associated symptoms, manifested as higher body weight, lower diarrhea scores, and longer colon length (Fig. 6B and C). IPA20 treatment restored redox homeostasis by enhancing SOD activity ( $P < 0.01$ ) and reducing MDA accumulation ( $P < 0.01$ ) (Fig. 6D). The protective mechanism of IPA was associated with a potent anti-inflammatory capacity, as it suppressed the elevation of IL-1 $\beta$ , TNF- $\alpha$ , and IL-17A in systemic circulation and IL-6, IL-1 $\beta$ , and TNF- $\alpha$  in colonic tissue (Fig. S6A and B). When compared to the PC group, HE and AB-PAS staining showed that mice administered with IPA maintained colonic epithelial integrity and abrogated the depletion of mucin-producing goblet cells in a dose-dependent manner (Fig. 6E and Fig. S6C). Furthermore, mice supplemented with IPA restored occludin localization at tight junctions (Fig. 6E) and upregulated mRNA expression levels of both occludin and claudin-1 (Fig. S6D), indicating amelioration of 5-FU-induced intestinal barrier damage. Moreover, mice administered with IPA exhibited substantially elevated intestinal expression levels of PXR and its target genes, Cyp3a11 and Abcb1a, relative to mice in the PC group (Fig. 6F). To verify that IPA exerts its protective effect *via* PXR activation, we performed experiments using Caco-2 cells. Caco-2 cell viability at different IPA concentrations is shown in Fig. 6G. Based on these results, a concentration of 50  $\mu$ M IPA was selected for subsequent intervention experiments. IPA administration reversed 5-FU-induced cellular damage, evidenced by decreased IL-6 and increased occludin expression, but this protection was abolished by the PXR antagonist KTZ (Fig. 6H). Mechanistically, IPA treatment elevated the expression of PXR (Fig. 6H) and its downstream targets CYP3A4 and ABCB1 (Fig. S6E), compared to 5-FU alone, an upregulation that was also blocked by KTZ.

## Discussion

In this study, we investigated the effects of *L. salivarius* Li01 on 5-FU-induced diarrhea in mice. Administration of 5-FU resulted in severe diarrheal symptoms, driven by elevated colonic inflammation, oxidative stress, intestinal barrier damage, and microbial dysbiosis. In contrast, Li01 treatment significantly ameliorated these pathological alterations. Further mechanistic investigation revealed that the gut microbiota and microbiota-derived IPA play an important role in mediating the protective effects of Li01 against 5-FU-triggered diarrhea.

The mechanism by which intestinal mucosal injury is caused by 5-FU has been extensively studied. The pathogenesis

of this condition is multifactorial; however, the direct cytotoxic effect of 5-FU on intestinal crypt cells serves as the primary initiating event.<sup>33</sup> Following intracellular conversion of 5-FU to fluorodeoxyuridine monophosphate, the metabolite potently and irreversibly inhibits thymidylate synthase (TS), resulting in impaired synthesis of deoxythymidine monophosphate (dTTP).<sup>34</sup> This critical metabolic disruption leads to defective DNA synthesis in intestinal epithelial cells and directly impedes the normal division and renewal of crypt stem cells.<sup>35</sup> Consequently, the regenerative process of the intestinal mucosa is severely compromised, culminating in the characteristic pathological findings of villous blunting and atrophy.<sup>36</sup> This primary insult triggers a complex cascade of molecular events, characterized by the upregulation of pro-inflammatory cytokines, the induction of profound oxidative stress, and the subsequent activation of apoptosis and necroptosis pathways.<sup>37</sup> Crucially, this damage disrupts the integrity of the intestinal mucosal barrier, facilitating bacterial translocation and sustaining a vicious cycle of inflammation and tissue injury.<sup>38</sup> While this pathophysiological framework is well-established, effective preventive or therapeutic strategies remain an unmet clinical need.

Transcriptome analysis revealed a significant suppression of the Th17 cell differentiation pathway in Li01-treated mice, contrasting with its activation in the 5-FU group. Given the established role of this pathway in intestinal inflammation, its downregulation could logically result in reduced production of related pro-inflammatory mediators.<sup>39,40</sup> Consistent with this possibility, we observed significantly lower levels of IL-1 $\beta$ , IL-6, TNF- $\alpha$ , and IL-17A in serum and colonic tissue following Li01 administration. Collectively, the alleviating effect of Li01 on 5-FU-induced diarrhea appear to be mediated *via* immune homeostasis. However, future studies directly quantifying Th17 cells and their key effector molecules are warranted to substantiate this mechanistic insight.

Emerging evidence indicates that the gut microbiota plays a significant role in human health. This is particularly evident in the context of intestinal pathologies, where microbial dysbiosis has been implicated in the pathogenesis of a range of disorders.<sup>41</sup> Our results showed that 5-FU induces a dramatic shift in the gut microbiota of mice by decreasing the proportion of Firmicutes and increasing the proportion of Bacteroidetes. This observed shift aligns with previous publications: a markedly reduced F/B ratio is a hallmark of intestinal inflammation, whereas an elevated ratio is frequently reported in obesity.<sup>42</sup> The increased relative abundance of Proteobacteria, a phylum encompassing numerous potential pathogens, indicates a shift toward a dysbiotic state that is often associated with intestinal inflammation.<sup>43</sup> In addition, Desulfovibrionaceae can convert sulfate into hydrogen sulfide (H<sub>2</sub>S), a genotoxic and pro-inflammatory metabolite that impairs colonocyte metabolism and disrupts the mucosal barrier.<sup>44</sup> Our study indicates that administration of Li01 restores the imbalanced microbial homeostasis in 5-FU-challenged mice; notably, Li01 appears to suppress the expansion of typical pathogen-like communities, including



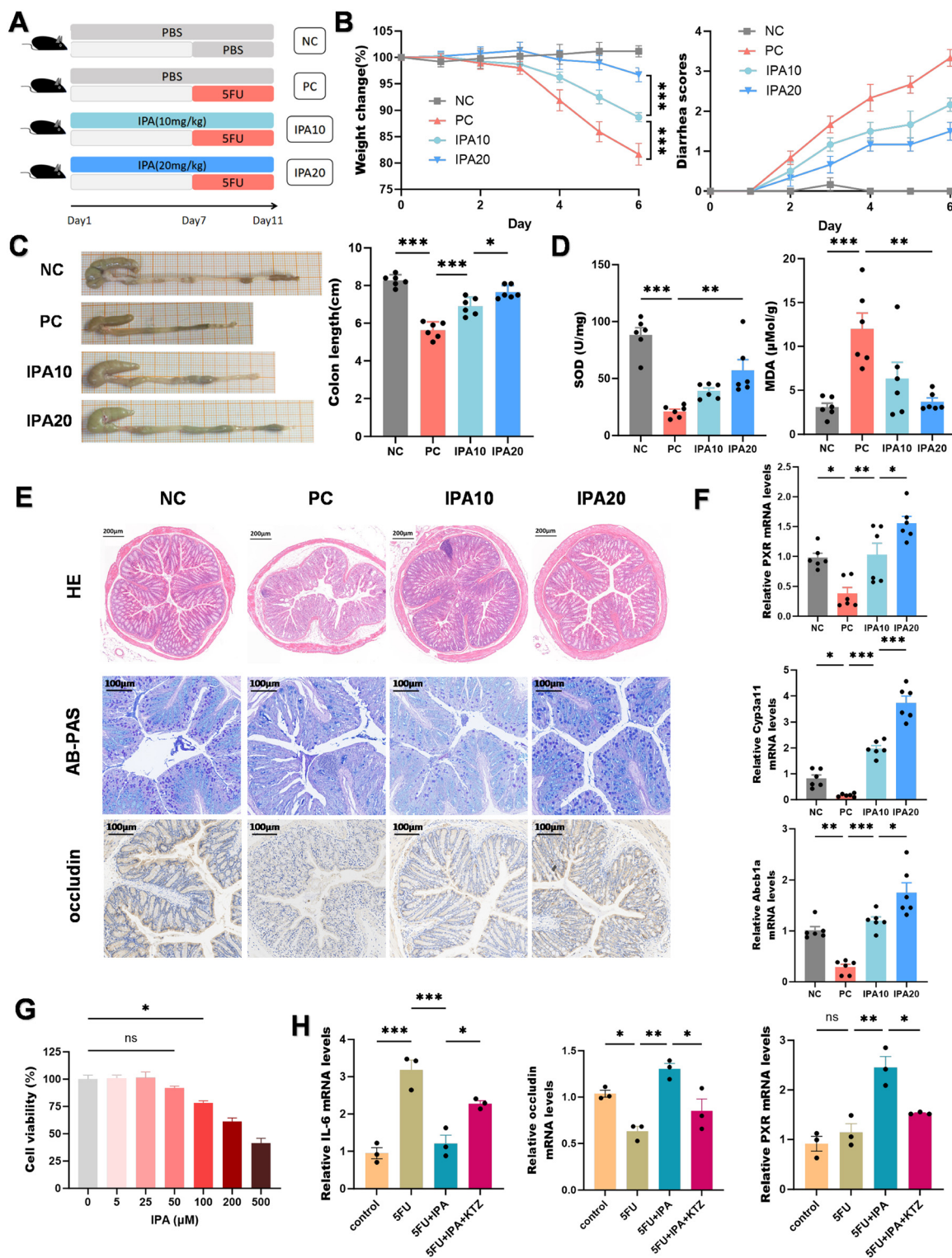


**Fig. 6** IPAmeliorated 5-FU-triggered diarrhea. (A) Study design of the indole-3-propionic acid supplement experiment. (B) Weight change and diarrhea scores of the four groups of mice. (C) Representative photos of the colon (left) and the colon length (right). (D) SOD activity and MDA content in colon tissues. (E) Representative images of HE staining, AB-PAS staining, and occludin immunohistochemical staining from colon tissues. (F) Colonic PXR, Cyp3a11, and Abcb1a expression levels. (G) Cell viability after treatment with IPA for 24 h. (H) Relative expression of IL-6, occludin, and PXR in Caco-2 cells. Data are presented as mean  $\pm$  SEM. ns,  $P > 0.05$ ,  $*P < 0.05$ ,  $**P < 0.01$ ,  $***P < 0.001$ .



Proteobacteria and Desulfovibrionaceae. *L. reuteri* and *L. johnsonii* are indispensable commensal microorganisms within the gut ecosystems of humans and animals. These species function as key commensals by orchestrating host immunity, reinforcing gut barrier integrity, and producing bioactive metabolites.<sup>45</sup> For example, *L. reuteri* stimulates intestinal epithelial proliferation and protects the mucosal barrier from inflammation by promoting Paneth cell expansion and upregulating the expression of antimicrobial peptides, including Defa1, Defa6, and Lyz-1.<sup>46</sup> *L. johnsonii* alleviates experimental colitis by promoting the polarization of resident macrophages toward an anti-inflammatory CD206<sup>+</sup> phenotype characterized by IL-10 production, mechanistically through the TLR1/2-STAT3 signaling pathway.<sup>47</sup> In our study, mice administered with Li01 showed significantly higher abundance of *L. reuteri* and *L. johnsonii*. This microbial shift was concomitant with elevated IL-10 levels, decreased pro-inflammatory cytokines, and improved intestinal barrier function, possibly suggesting a potential mechanistic link between the enrichment of these specific *Lactobacilli* and the observed amelioration. To establish a causal link, we utilized an antibiotic-treated mouse model in which the endogenous gut microbiota was substantially depleted. The absence of an ameliorative effect of Li01 in 5-FU-treated antibiotic mice verifies that the intestinal microbiome is essential in mediating the beneficial effects of Li01 against mucositis. Thus, we propose that Li01 initiates a protective host response by modulating the gut microbial community, which in turn mitigates 5-FU-induced diarrhea.

It is being increasingly recognized that metabolites generated by the gut microbiota serve as pivotal signal mediators within microbial ecosystems and in the dialogue between the host and the microbiota.<sup>48</sup> Thus, the identification and functional characterization of these microbial metabolites are essential for advancing our understanding of microbiota functionality and the dynamic relationships between the host and microbiota.<sup>49</sup> IPA is a tryptophan-derived metabolite synthesized by specific commensal bacteria in the gut through enzymatic processes.<sup>50</sup> Due to the beneficial properties of the compound, including functioning as an antioxidant and immunomodulator, a substantial amount of research has established the pivotal role of IPA in regulating host metabolism. For instance, IPA has been shown to promote apoptosis of mucosal Th1/Th17 cells and alleviate inflammatory bowel disease by binding to heat shock protein 70 (HSP70).<sup>51</sup> Gut microbiota-derived IPA ameliorates diabetic kidney disease by inhibiting ubiquitin-mediated degradation of SIRT1.<sup>52</sup> However, the role of IPA in 5-FU-induced mucositis remains largely unexplored. Our results demonstrated that Li01 administration alleviated 5-FU-related diarrhea, whereas this protective effect was absent after antibiotic administration. This indicates that bioactive metabolites derived from the gut microbiome are essential for protection against mucositis. Metabolomic analysis identified IPA as a central mediator in the protective mechanism of Li01. Following antibiotic-induced microbiota depletion, IPA levels in the feces and

serum of Li01-treated mice did not show an increase, linking the maintenance of host IPA homeostasis directly to an intact gut microbiota. Li01 administration markedly increased the abundance of *L. reuteri* and *L. johnsonii* in normal mice, but did not increase their abundance in antibiotic-treated mice. Then, a strong positive correlation between IPA levels and the relative abundance of *L. reuteri* and *L. johnsonii* was observed. Importantly, our *in vitro* co-culture experiments substantiate this link: while neither Li01, *L. reuteri*, nor *L. johnsonii* alone metabolized tryptophan into IPA, co-cultures of Li01 with either *L. reuteri* or *L. johnsonii* resulted in significant IPA production. This result explicitly demonstrates that the enrichment of *L. reuteri* and *L. johnsonii*, in conjunction with Li01, is both necessary and sufficient for the observed rise in IPA. This aligns with previous research demonstrating a positive correlation between IPA and *L. reuteri*.<sup>53</sup> And earlier studies have indicated that while *L. johnsonii* alone metabolizes tryptophan only to indole-3-lactic acid (ILA), it collaborates with *Clostridium sporogenes* to facilitate IPA production.<sup>54</sup> Collectively, these data support that Li01 promotes the growth of *L. reuteri* and *L. johnsonii*, which in turn collaborate with Li01 itself to drive IPA synthesis. Therefore, we propose that the protective effect of Li01 is mediated, at least in part, by its ability to foster a microbial environment that enriches IPA-producing symbionts like *L. reuteri* and *L. johnsonii*, thereby driving the increase in this key protective metabolite.

Previous studies have shown that IPA mediates protection through different mechanisms; some reports indicate that IPA functions through activation of the aryl hydrocarbon receptor (AhR), while others have shown that it acts *via* the pregnane X receptor (PXR).<sup>55,56</sup> Our findings associate its benefits in 5-FU-induced mucositis with PXR activation. Mechanistically, IPA treatment elevated intestinal expression of PXR and its target genes, Cyp3a11 and Abcb1a.<sup>57</sup> The induction of these genes is critically linked to the observed phenotypic improvement. Cyp3a11 is involved in detoxification processes that may reduce oxidative stress, while Abcb1a is an efflux transporter known to maintain barrier integrity and modulate inflammatory responses by exporting toxins and xenobiotics.<sup>58,59</sup> IPA, through its activation of PXR and subsequent upregulation of its target genes Cyp3a11 and Abcb1a, provides a direct molecular pathway connecting metabolite signaling to the alleviation of barrier dysfunction, inflammation, and oxidative stress.

Our demonstration that oral gavage of IPA effectively ameliorates 5-FU-induced intestinal damage provides a promising first step in evaluating its therapeutic potential *via* a clinically feasible route. However, a deeper understanding of its *in vivo* pharmacokinetic profile is essential for further translation. Although oral administration proved effective in our model, a direct comparative pharmacokinetic and pharmacodynamic study against systemic administration is warranted. Such a study would help clarify the dominant mode of action and define the most efficient delivery route. Furthermore, employing isotope-labeled IPA might enable precise tracking of its absorption and distribution, which would be a key objective in



future studies.<sup>60</sup> Future delivery strategies, such as enteric coating, lipid-based nano-carriers, or co-administration with absorption enhancers, could be explored to improve intestinal stability and enhance epithelial uptake of IPA.<sup>61,62</sup> Ultimately, while our work validates the oral activity of IPA, dedicated pharmacokinetic studies and systematic route comparisons constitute the logical and necessary next steps to translate this gut microbiota-derived metabolite into a targeted and efficient therapeutic agent.

Although this study demonstrates that Li01 ameliorates 5-FU-induced diarrhea in mice through the gut bacterial metabolite IPA, several limitations must be acknowledged. First, the exact *in vivo* mechanism responsible for the synthesis of IPA has not been fully elucidated. Second, since administration of Li01 was associated with substantial changes in the gut microbiota and metabolome, contributions of other microbiota and metabolites to the observed effects cannot be ruled out. Third, the beneficial effects exerted by Li01 and IPA were validated only in mice, and their effects in humans remain unclear. Thus, further studies are essential to decipher the precise mechanisms by which probiotics modulate the microbiota–metabolite–host crosstalk.

## Conclusion

We found that Li01 administration alleviated 5-FU-triggered diarrhea by mitigating colonic inflammation, oxidative stress, and barrier damage in a gut microbiota-dependent manner. Mechanistically, administration of Li01 ameliorated microbial imbalance and significantly enriched the gut microbiota-derived metabolite IPA. Furthermore, IPA could activate PXR and contribute to the protection against intestinal mucositis caused by 5-FU. Additionally, we discovered that IPA production was mediated by cooperation between Li01 and either *L. reuteri* or *L. johnsonii*. Our study highlights the significance of the Li01–microbiota–IPA axis, suggesting that both the probiotic Li01 and the metabolite IPA may be promising therapeutic candidates for the prevention and mitigation of 5-FU-induced diarrhea. Future research will further elucidate the detailed mechanisms of this axis and evaluate the therapeutic potential of Li01 in clinical scenarios.

## Author contributions

Pengyu Yin: conceptualization, investigation, writing – original draft, and visualization. Bo Qiu: data curation, investigation, and visualization. Lwuan Xu: data curation and methodology. Siyuan Xie: investigation and validation. Shuobo Zhang: investigation and software. Jingyi Zhang: methodology. Björn Berglund: writing – review & editing. Mingfei Yao: writing – review & editing, funding acquisition, and supervision. Lanjuan Li: funding acquisition, supervision, conceptualization, and writing – review & editing.

## Conflicts of interest

The authors declare no competing interests.

## Data availability

All data of this study are presented in the paper or the supplementary information (SI). Supplementary information is available. See DOI: <https://doi.org/10.1039/d6fo00050a>.

Additional data relevant to the article are available from the corresponding author upon request.

## Acknowledgements

This study was supported by the National Natural Science Foundation of China (32372339), the National Key Research and Development Program of China (2022YFA1303801), the Fundamental Research Funds for the Central Universities (2025ZFJH03), the Central Guidance Fund for Local Science and Technology Development (2024ZY01054), and the Shandong Provincial Laboratory Project (JNL-2025012B).

## References

- 1 C. H. Lin, W. P. Jiang, N. Itokazu and G. J. Huang, Chlorogenic acid attenuates 5-fluorouracil-induced intestinal mucositis in mice through SIRT1 signaling-mediated oxidative stress and inflammatory pathways, *Biomed. Pharmacother.*, 2025, **186**, 117982.
- 2 T. A. Scott, L. M. Quintaneiro, P. Norvaisas, P. P. Lui, M. P. Wilson, K. Y. Leung, *et al.*, Host-Microbe Co-metabolism Dictates Cancer Drug Efficacy in *C. elegans*, *Cell*, 2017, **169**(3), 442–456.
- 3 C. G. Moertel, T. R. Fleming, J. S. Macdonald, D. G. Haller, J. A. Laurie, C. M. Tangen, *et al.*, Fluorouracil plus levamisole as effective adjuvant therapy after resection of stage III colon carcinoma: a final report, *Ann. Intern. Med.*, 1995, **122**(5), 321–326.
- 4 K. J. Chen, Y. L. Chen, S. H. Ueng, T. L. Hwang, L. M. Kuo and P. W. Hsieh, Neutrophil elastase inhibitor (MPH-966) improves intestinal mucosal damage and gut microbiota in a mouse model of 5-fluorouracil-induced intestinal mucositis, *Biomed. Pharmacother.*, 2021, **134**, 111152.
- 5 H. R. Wardill, J. M. Bowen and R. J. Gibson, New pharmacotherapy options for chemotherapy-induced alimentary mucositis, *Expert Opin. Biol. Ther.*, 2014, **14**(3), 347–354.
- 6 M. Yasuda, S. Kato, N. Yamanaka, M. Iimori, K. Matsumoto, D. Utsumi, *et al.*, 5-HT<sub>3</sub> receptor antagonists ameliorate 5-fluorouracil-induced intestinal mucositis by suppression of apoptosis in murine intestinal crypt cells, *Br. J. Pharmacol.*, 2013, **168**(6), 1388–1400.
- 7 L. Wang, R. Wang, G. Y. Wei, S. M. Wang and G. H. Du, Dihydrotanshinone attenuates chemotherapy-induced



- intestinal mucositis and alters fecal microbiota in mice, *Biomed. Pharmacother.*, 2020, **128**, 110262.
- 8 C. L. Boulangé, A. L. Neves, J. Chilloux, J. K. Nicholson and M. E. Dumas, Impact of the gut microbiota on inflammation, obesity, and metabolic disease, *Genome Med.*, 2016, **8**(1), 42.
  - 9 J. Xia, W. Guo, M. Hu, X. Jin, S. Zhang, B. Liu, *et al.*, Resynchronized rhythmic oscillations of gut microbiota drive time-restricted feeding induced nonalcoholic steatohepatitis alleviation, *Gut Microbes*, 2023, **15**(1), 2221450.
  - 10 H. L. Li, L. Lu, X. S. Wang, L. Y. Qin, P. Wang, S. P. Qiu, *et al.*, Alteration of Gut Microbiota and Inflammatory Cytokine/Chemokine Profiles in 5-Fluorouracil Induced Intestinal Mucositis, *Front. Cell. Infect. Microbiol.*, 2017, **7**, 455.
  - 11 A. B. Santana, B. S. Souto, N. C. M. Santos, J. A. Pereira, C. A. Tagliati, R. D. Novaes, *et al.*, Murine response to the opportunistic bacterium *Pseudomonas aeruginosa* infection in gut dysbiosis caused by 5-fluorouracil chemotherapy-induced mucositis, *Life Sci.*, 2022, **307**, 120890.
  - 12 D. Tang, R. Qiu, X. Qiu, M. Sun, M. Su, Z. Tao, *et al.*, Dietary restriction rescues 5-fluorouracil-induced lethal intestinal toxicity in old mice by blocking translocation of opportunistic pathogens, *Gut Microbes*, 2024, **16**(1), 2355693.
  - 13 C. Hill, F. Guarner, G. Reid, G. R. Gibson, D. J. Merenstein, B. Pot, *et al.*, Expert consensus document. The International Scientific Association for Probiotics and Prebiotics consensus statement on the scope and appropriate use of the term probiotic, *Nat. Rev. Gastroenterol. Hepatol.*, 2014, **11**(8), 506–514.
  - 14 W. Yang and Y. Cong, Gut microbiota-derived metabolites in the regulation of host immune responses and immune-related inflammatory diseases, *Cell. Mol. Immunol.*, 2021, **18**(4), 866–877.
  - 15 Y. Wu, S. Li, L. Lv, S. Jiang, L. Xu, H. Chen, *et al.*, Protective effect of *Pediococcus pentosaceus* Li05 on diarrhea-predominant irritable bowel syndrome in rats, *Food Funct.*, 2024, **15**(7), 3692–3708.
  - 16 Z. P. Zou, Y. Du, T. T. Fang, Y. Zhou and B. C. Ye, Biomarker-responsive engineered probiotic diagnoses, records, and ameliorates inflammatory bowel disease in mice, *Cell Host Microbe*, 2023, **31**(2), 199–212.
  - 17 M. Hu, X. Wu, M. Luo, H. Wei, D. Xu and F. Xu, *Lactobacillus rhamnosus* FLRH93 protects against intestinal damage in mice induced by 5-fluorouracil, *J. Dairy Sci.*, 2020, **103**(6), 5003–5018.
  - 18 L. M. Tavares, L. C. L. de Jesus, V. L. Batista, F. A. L. Barroso, A. Dos Santos Freitas, G. M. Campos, *et al.*, Synergistic synbiotic containing fructooligosaccharides and *Lactobacillus delbrueckii* CIDCA 133 alleviates chemotherapy-induced intestinal mucositis in mice, *World J. Microbiol. Biotechnol.*, 2023, **39**(9), 235.
  - 19 B. Qiu, L. Zhu, S. Zhang, S. Han, Y. Fei, F. Ba, *et al.*, Prevention of Loperamide-Induced Constipation in Mice and Alteration of 5-Hydroxytryptamine Signaling by *Ligilactobacillus salivarius* Li01, *Nutrients*, 2022, **14**(19), 4083.
  - 20 L. Yang, X. Bian, W. Wu, L. Lv, Y. Li, J. Ye, *et al.*, Protective effect of *Lactobacillus salivarius* Li01 on thioacetamide-induced acute liver injury and hyperammonaemia, *Microb. Biotechnol.*, 2020, **13**(6), 1860–1876.
  - 21 Y. Yuan, J. Yang, A. Zhuge, L. Li and S. Ni, Gut microbiota modulates osteoclast glutathione synthesis and mitochondrial biogenesis in mice subjected to ovariectomy, *Cell Proliferation*, 2022, **55**(3), e13194.
  - 22 H. Sakai, A. Sagara, K. Matsumoto, A. Jo, A. Hirosaki, K. Takase, *et al.*, Neutrophil recruitment is critical for 5-fluorouracil-induced diarrhea and the decrease in aquaporins in the colon, *Pharmacol. Res.*, 2014, **87**, 71–79.
  - 23 J. Xia, S. Jiang, L. Lv, W. Wu, Q. Wang, Q. Xu, *et al.*, Modulation of the immune response and metabolism in germ-free rats colonized by the probiotic *Lactobacillus salivarius* LI01, *Appl. Microbiol. Biotechnol.*, 2021, **105**(4), 1629–1645.
  - 24 T. Wang, B. Chen, M. Luo, L. Xie, M. Lu, X. Lu, *et al.*, Microbiota-indole 3-propionic acid-brain axis mediates abnormal synaptic pruning of hippocampal microglia and susceptibility to ASD in IUGR offspring, *Microbiome*, 2023, **11**(1), 245.
  - 25 Y. Fei, S. Zhang, S. Han, B. Qiu, Y. Lu, W. Huang, *et al.*, The Role of Dihydroresveratrol in Enhancing the Synergistic Effect of *Ligilactobacillus salivarius* Li01 and Resveratrol in Ameliorating Colitis in Mice, *Research*, 2022, **2022**, 9863845.
  - 26 G. Mazzocchi, T. Colangelo, A. Panza, R. Rubino, A. De Cata, C. Tiberio, *et al.*, Deregulated expression of cryptochrome genes in human colorectal cancer, *Mol. Cancer*, 2016, **15**, 6.
  - 27 G. Esposito, N. Nobile, S. Gigli, L. Seguella, M. Pesce, A. d'Alessandro, *et al.*, Rifaximin Improves Clostridium difficile Toxin A-Induced Toxicity in Caco-2 Cells by the PXR-Dependent TLR4/MyD88/NF-κB Pathway, *Front. Pharmacol.*, 2016, **7**, 120.
  - 28 L. Huang, Y. Wu, Y. Fan, Y. Su, Z. Liu, J. Bai, *et al.*, The growth-promoting effects of protein hydrolysates and their derived peptides on probiotics: structure-activity relationships, mechanisms and future perspectives, *Crit. Rev. Food Sci. Nutr.*, 2025, **65**(22), 4401–4420.
  - 29 F. Ba, W. Wang, Y. Huang, S. Zhang, B. Qiu, S. Xie, *et al.*, Improving fecal transplantation precision for enhanced maturation of intestinal function in germ-free mice through microencapsulation and probiotic intervention, *Microbiome*, 2025, **13**(1), 212.
  - 30 S. Li, A. Zhuge, H. Chen, S. Han, J. Shen, K. Wang, *et al.*, Sedanolide alleviates DSS-induced colitis by modulating the intestinal FXR-SMPD3 pathway in mice, *J. Adv. Res.*, 2025, **69**, 413–426.
  - 31 S. Li, A. Zhuge, J. Xia, S. Wang, L. Lv, K. Wang, *et al.*, *Bifidobacterium longum* R0175 protects mice against APAP-induced liver injury by modulating the Nrf2 pathway, *Free Radical Biol. Med.*, 2023, **203**, 11–23.



- 32 Y. Luo, Y. Hao, C. Sun, Z. Lu, H. Wang, Y. Lin, *et al.*, Gut-derived indole propionic acid alleviates liver fibrosis by targeting profibrogenic macrophages via the gut-liver axis, *Cell. Mol. Immunol.*, 2025, **22**(11), 1414–1426.
- 33 G. Naren, J. Guo, Q. Bai, N. Fan and B. Nashun, Reproductive and developmental toxicities of 5-fluorouracil in model organisms and humans, *Expert Rev. Mol. Med.*, 2022, **24**, e9.
- 34 D. B. Longley, D. P. Harkin and P. G. Johnston, 5-fluorouracil: mechanisms of action and clinical strategies, *Nat. Rev. Cancer*, 2003, **3**(5), 330–338.
- 35 J. K. Chen, K. A. Merrick, Y. W. Kong, A. Izrael-Tomasevic, G. Eng, E. D. Handly, *et al.*, An RNA damage response network mediates the lethality of 5-FU in colorectal cancer, *Cell Rep. Med.*, 2024, **5**(10), 101778.
- 36 K. Ishikawa, S. Sugimoto, M. Oda, M. Fujii, S. Takahashi, Y. Ohta, *et al.*, Identification of Quiescent LGR5(+) Stem Cells in the Human Colon, *Gastroenterology*, 2022, **163**(5), 1391–1406.
- 37 S. Blondy, V. David, M. Verdier, M. MATHONNET, A. Perraud and N. Christou, 5-Fluorouracil resistance mechanisms in colorectal cancer: From classical pathways to promising processes, *Cancer Sci.*, 2020, **111**(9), 3142–3154.
- 38 K. R. Trepka, W. A. Kidder, T. S. Kyaw, T. Halsey, C. A. Olson, E. F. Ortega, *et al.*, Expansion of a bacterial operon during cancer treatment ameliorates fluoropyrimidine toxicity, *Sci. Transl. Med.*, 2025, **17**(794), eadq8870.
- 39 M. Alexander, Q. Y. Ang, R. R. Nayak, A. E. Bustion, M. Sandy, B. Zhang, *et al.*, Human gut bacterial metabolism drives Th17 activation and colitis, *Cell Host Microbe*, 2022, **30**(1), 17–30.
- 40 L. Huangfu, R. Li, Y. Huang and S. Wang, The IL-17 family in diseases: from bench to bedside, *Signal Transduction Targeted Ther.*, 2023, **8**(1), 402.
- 41 R. M. Jones and A. S. Neish, Gut Microbiota in Intestinal and Liver Disease, *Annu. Rev. Phytopathol.*, 2021, **16**, 251–275.
- 42 N. Vallianou, G. S. Christodoulatos, I. Karampela, D. Tsilingiris, F. Magkos, T. Stratigou, *et al.*, Understanding the Role of the Gut Microbiome and Microbial Metabolites in Non-Alcoholic Fatty Liver Disease: Current Evidence and Perspectives, *Biomolecules*, 2021, **12**(1), 56.
- 43 S. Umeda, T. Sujino, K. Miyamoto, Y. Yoshimatsu, Y. Harada, K. Nishiyama, *et al.*, D-amino Acids Ameliorate Experimental Colitis and Cholangitis by Inhibiting Growth of Proteobacteria: Potential Therapeutic Role in Inflammatory Bowel Disease, *Cell. Mol. Gastroenterol. Hepatol.*, 2023, **16**(6), 1011–1031.
- 44 Q. Qi, H. Zhang, Z. Jin, C. Wang, M. Xia, B. Chen, *et al.*, Hydrogen sulfide produced by the gut microbiota impairs host metabolism via reducing GLP-1 levels in male mice, *Nat. Metab.*, 2024, **6**(8), 1601–1615.
- 45 A. B. Shah, A. Baiseitova, M. Zahoor, I. Ahmad, M. Ikram, A. Bakhsh, *et al.*, Probiotic significance of *Lactobacillus* strains: a comprehensive review on health impacts, research gaps, and future prospects, *Gut Microbes*, 2024, **16**(1), 2431643.
- 46 H. Wu, S. Xie, J. Miao, Y. Li, Z. Wang, M. Wang, *et al.*, *Lactobacillus reuteri* maintains intestinal epithelial regeneration and repairs damaged intestinal mucosa, *Gut Microbes*, 2020, **11**(4), 997–1014.
- 47 D. J. Jia, Q. W. Wang, Y. Y. Hu, J. M. He, Q. W. Ge, Y. D. Qi, *et al.*, *Lactobacillus johnsonii* alleviates colitis by TLR1/2-STAT3 mediated CD206(+) macrophages(IL-10) activation, *Gut Microbes*, 2022, **14**(1), 2145843.
- 48 K. A. Krautkramer, J. Fan and F. Bäckhed, Gut microbial metabolites as multi-kingdom intermediates, *Nat. Rev. Microbiol.*, 2021, **19**(2), 77–94.
- 49 M. G. Rooks and W. S. Garrett, Gut microbiota, metabolites and host immunity, *Nat. Rev. Immunol.*, 2016, **16**(6), 341–352.
- 50 A. K. Sinha, M. F. Laursen, J. E. Brinck, M. L. Rybtke, A. P. Hjørne, N. Procházková, *et al.*, Dietary fibre directs microbial tryptophan metabolism via metabolic interactions in the gut microbiota, *Nat. Metab.*, 2024, **9**(8), 1964–1978.
- 51 H. Gao, M. Sun, A. Li, Q. Gu, D. Kang, Z. Feng, *et al.*, Microbiota-derived IPA alleviates intestinal mucosal inflammation through upregulating Th1/Th17 cell apoptosis in inflammatory bowel disease, *Gut Microbes*, 2025, **17**(1), 2467235.
- 52 Y. Zeng, M. Guo, Q. Wu, X. Tan, C. Jiang, F. Teng, *et al.*, Gut microbiota-derived indole-3-propionic acid alleviates diabetic kidney disease through its mitochondrial protective effect via reducing ubiquitination mediated-degradation of SIRT1, *J. Adv. Res.*, 2025, **73**, 607–630.
- 53 S. Heumel, V. de Rezende Rodvalho, C. Urien, F. Specque, P. Brito Rodrigues, C. Robil, *et al.*, Shotgun metagenomics and systemic targeted metabolomics highlight indole-3-propionic acid as a protective gut microbial metabolite against influenza infection, *Gut Microbes*, 2024, **16**(1), 2325067.
- 54 D. Jia, Q. Wang, Y. Qi, Y. Jiang, J. He, Y. Lin, *et al.*, Microbial metabolite enhances immunotherapy efficacy by modulating T cell stemness in pan-cancer, *Cell*, 2024, **187**(7), 1651–1665.
- 55 R. Peng, C. Song, S. Gou, H. Liu, H. Kang, Y. Dong, *et al.*, Gut *Clostridium sporogenes*-derived indole propionic acid suppresses osteoclast formation by activating pregnane X receptor, *Pharmacol. Res.*, 2024, **202**, 107121.
- 56 H. Shao, F. Min, T. Bai, Z. Wang, Y. Liu, F. Yang, *et al.*, *Bifidobacterium breve* M-16 V Alleviates Cow's Milk Allergy in a Mouse Model via Gut Microbiota-Derived Indole-3-Propionic Acid-Aryl Hydrocarbon Receptor Signaling Axis, *Allergy*, 2025, DOI: [10.1111/all.16684](https://doi.org/10.1111/all.16684).
- 57 A. Kamiya, Y. Inoue and F. J. Gonzalez, Role of the hepatocyte nuclear factor 4alpha in control of the pregnane X receptor during fetal liver development, *Hepatology*, 2003, **37**(6), 1375–1384.
- 58 X. Qin and X. Wang, Role of vitamin D receptor in the regulation of CYP3A gene expression, *Acta Pharm. Sin. B*, 2019, **9**(6), 1087–1098.



- 59 M. L. Chen, X. Huang, H. Wang, C. Hegner, Y. Liu, J. Shang, *et al.*, CAR directs T cell adaptation to bile acids in the small intestine, *Nature*, 2021, **593**(7857), 147–151.
- 60 Y. Zhao, P. Yang, Y. Shencheng, S. Li, M. Zhou, M. Gao, *et al.*, Tropomyosin-targeted LC-MS/MS for quantitative detection of molluscan allergens in foods: Method validation and application, *Food Chem.*, 2026, **507**, 148239.
- 61 J. Ye, H. Sun, Q. Zhang, J. He and M. Zhou, Microalgae-based Intestinal villi-targeting multistage biosystem for irritable bowel syndrome treatment, *Nat. Commun.*, 2025, **16**(1), 7614.
- 62 Y. Lee, Y. Kim, S. Kwon, O. K. Park, G. H. Min, J. Chu, *et al.*, Orally Administered Nanoparticle Coacervate for Therapeutic Coating of Full Gastrointestinal Tract, *Adv. Biomater.*, 2026, e14708.

